

Case report

Pulmonary extranodal marginal zone lymphoma that presented with macroglobulinemia and marked plasmacytic cell proliferation carrying the t(14;18)(q32;q21)/*MALTI*-immunoglobulin heavy-chain fusion gene in pleural fluid

Takashi Akasaka,¹⁾ Chiyuki Kishimori,²⁾ Fumiyo Maekawa,²⁾ Kayo Takeoka,²⁾
Masahiko Hayashida,²⁾ Hiroshi Gomyo,³⁾ Tohru Murayama,³⁾ and Hitoshi Ohno^{1),2)}

An 80-year-old man presented with the accumulation of pleural fluid in the right thoracic cavity. Serum electrophoresis revealed an M-component and immunofixation confirmed IgM/λ. The level of IgM was 1,526 mg/dL. Imaging studies showed an infiltrative condition of the ipsilateral lung parenchyma. The fluid contained abundant neoplastic cells with the morphological and immunophenotypic features of plasma cells, which expressed IgM/λ monoclonal immunoglobulins on the cell surface and in the cytoplasm. The karyotype was 48,XY,+3,add(9)(p13),+12,add(14)(q32),del(16)(q22),-18,+mar, and a series of fluorescence *in situ* hybridization studies demonstrated that the add(14) chromosome represented der(14)t(14;18)(q32;q21), at which the *MALTI*-immunoglobulin heavy-chain (*IGH*) fusion gene was localized. A long-distance polymerase chain reaction amplified the fragment encompassing the two genes, showing that the junction occurred at the J6 segment of *IGH* and 3.7-kb upstream of the *MALTI* breakpoint cluster. We propose that this case represents an extreme form of the plasmacytic differentiation of extranodal marginal zone lymphoma that developed in the lung.

Keywords: macroglobulinemia, extranodal marginal zone lymphoma, plasmacytic differentiation, t(14;18)(q32;q32)/*MALTI*-*IGH* fusion gene

INTRODUCTION

Waldenström macroglobulinemia (WM) is a distinct clinicopathological disease entity showing lymphoplasmacytic lymphoma (LPL) in bone marrow and the IgM monoclonal protein in serum (i.e., macroglobulinemia) at any concentration.^{1,2} WM/LPL is characterized by the proliferation of small lymphocytes admixed with variable numbers of plasma cells and plasmacytoid lymphocytes.² Patients with WM/LPL present with a number of symptoms attributable to tumor cell proliferation and/or an excess of macroglobulin. However, macroglobulinemia is observed not only in WM/LPL, but also a wide range of B-cell lymphoproliferative disorders, including extranodal marginal zone lymphoma (EMZL) of mucosa-associated lymphoid tissue (MALT lymphoma).³⁻⁵ EMZL/MALT lymphoma is composed of morphologically heterogeneous small B cells and the plasmacytic differentiation of lymphoma cells is common.⁴ Thus, the


distinction between WM/LPL and EMZL/MALT lymphoma showing plasmacytic differentiation and associated with the serum IgM monoclonal protein is not necessarily clear, even though >90% cases of the former disease have the *MYD88* P265P somatic mutation.^{2,6}

We herein describe a patient who presented with macroglobulinemia and the accumulation of pleural fluid in the unilateral thoracic cavity. Neoplastic cells in the fluid showed the cytomorphological and immunophenotypic features of plasma cells, indicating the differential diagnosis between WM/LPL and EMZL/MALT lymphoma. Cytogenetic and molecular studies demonstrated a translocation and fusion gene, which was exclusively associated with the latter disease.

Received: April 8, 2018. Revised: June 15, 2018. Accepted: July 6, 2018. J-STAGE Advance Published: August 8, 2018
DOI:10.3960/jslrt.18013

¹⁾Department of Hematology, Tenri Hospital, Nara Japan, ²⁾Tenri Institute of Medical Science, Nara Japan, and ³⁾Hematology Division, Department of Medicine, Hyogo Cancer Center, Hyogo, Japan

Corresponding author: Takashi Akasaka, MD, PhD, Department of Hematology, Tenri Hospital, 200 Mishima, Tenri, Nara 632-8552, Japan. E-mail: akasaka@tenriyorozu.jp
Copyright © 2018 The Japanese Society for Lymphoreticular Tissue Research

 This work is licensed under a Creative Commons Attribution-NonCommercial-ShareAlike 4.0 International License.

CASE REPORT

Case presentation

An 80-year-old man, who had been treated in another hospital for the recurrent accumulation of pleural fluid in the right thoracic cavity for 2 years, was referred to our department because a cytological examination of the fluid suggested lymphoma cells. On examination, breath sounds were decreased in the right hemithorax. There was no surface lymphadenopathy or hepatosplenomegaly. Oxygen saturation was 96% in room air. A chest radiograph showed prominent pleural effusion (Figure 1A). His hemoglobin level was 12.5 g/dL, white blood cell count was $6.95 \times 10^3/\mu\text{L}$, and platelet count was $289 \times 10^3/\mu\text{L}$. Total serum protein was 6.7 g/dL, albumin 3.2 g/dL, globulin 3.5 g/dL, lactate dehydrogenase 307 IU/L, higher than the normal range of 124 to 222 IU/L, creatinine 0.6 mg/dL, and C-reactive protein 2.25 mg/dL. Serum protein electrophoresis revealed an M-component migrating in the γ globulin area and immunofixation confirmed the IgM/ λ M protein. No urinary Bence Jones protein was detected. The level of IgG was 723 mg/dL, IgA was 83 mg/dL, and IgM was 1,526 mg/dL (normal range, 33 to 183 mg/dL). Serum free light-chain κ (FLC- κ) was 16.1 mg/L, FLC- λ was 20.5 mg/L, and the κ/λ ratio was 0.79. Soluble interleukin 2 receptor was 3,051 U/mL.

Computed tomography (CT) of the chest revealed the accumulation of pleural fluid in the right thoracic cavity in association with atelectasis of the middle and lower lobes, where the marked accumulation of the tracer was demonstrated by ^{18}F -fluorodeoxyglucose-positron emission tomography (FDG-PET) combined with CT (Figure 1B), suggesting that the atelectatic lesion contained an infiltrative

condition.

Thoracentesis yielded exudative fluid containing abundant neoplastic cells with the morphological features of plasma cells at a concentration of 6.13×10^3 cells per microliter (Figure 2A). These cells expressed IgM/ λ monoclonal immunoglobulins both on the cell surface and in the cytoplasm, and showed a wide range of expression levels of CD20, CD22, CD23, CD38, and CD138. CD19 and CD45RA were positive, and CD5, CD10, CD21, CD24, CD56, and surface IgD were negative (Figures 2B and C). The DNA index was 1.06 from normal diploid cells. Bone marrow showed hypercellularity containing CD20-positive plasma cells, and flow cytometry revealed a lymphoplasmacytic population with an identical immunophenotype to that of pleural fluid cells. Tests for the *MYD88* L265P somatic mutation were negative (Supplementary Figure S1).

Cytogenetic studies

The G-banding of metaphase spreads obtained from a short-term culture of pleural fluid cells demonstrated numerical and structural abnormalities, including a 14q+ chromosome and uncharacterized small marker chromosome; the karyotype according to the ISCN 2016 was 48,XY,+3,add(9)(p13),+12,add(14)(q32),del(16)(q22),-18,+mar (Figure 3A). Fluorescence *in situ* hybridization (FISH) of interphase nuclei with the *MYC*, *BCL2*, and *BCL6* dual-color, break-apart probes detected no rearrangement of these 3 genes, while nuclei carried 3 hybridization signals of *BCL2* and *BCL6* (Supplementary Figure S2). The hybridization of metaphase cells with the *BCL2-IGH* dual-color dual-fusion probe showed that the add(14) chromosome was marked by the *IGH* and *BCL2* probes (Figure 3B); however, these probes did not generate a fusion signal (Supplementary

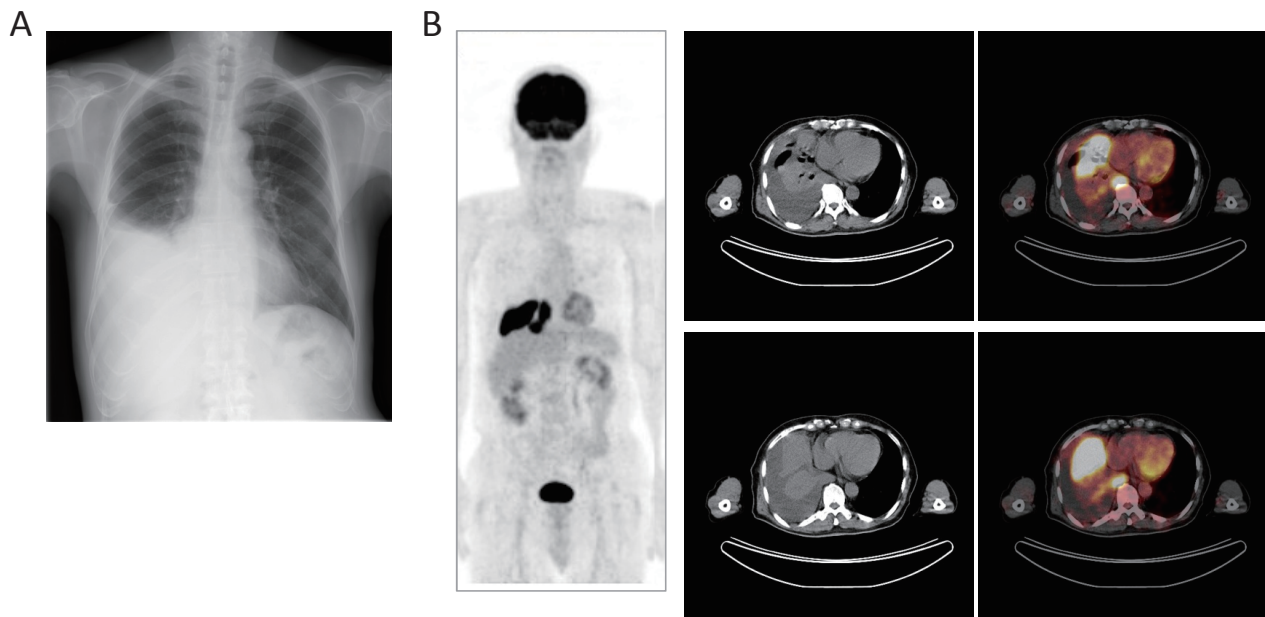


Fig. 1. Imaging studies showing pleural effusion of the right thoracic cavity and an infiltrative condition of the lung parenchyma. (A) Postero-anterior chest X-ray. (B) FDG-PET/CT. The anterior view of a maximum intensity projection image (*left*) and representative axial images of the thorax (*right*) are shown. The maximum standardized uptake value of the pulmonary lesion was 17.89.

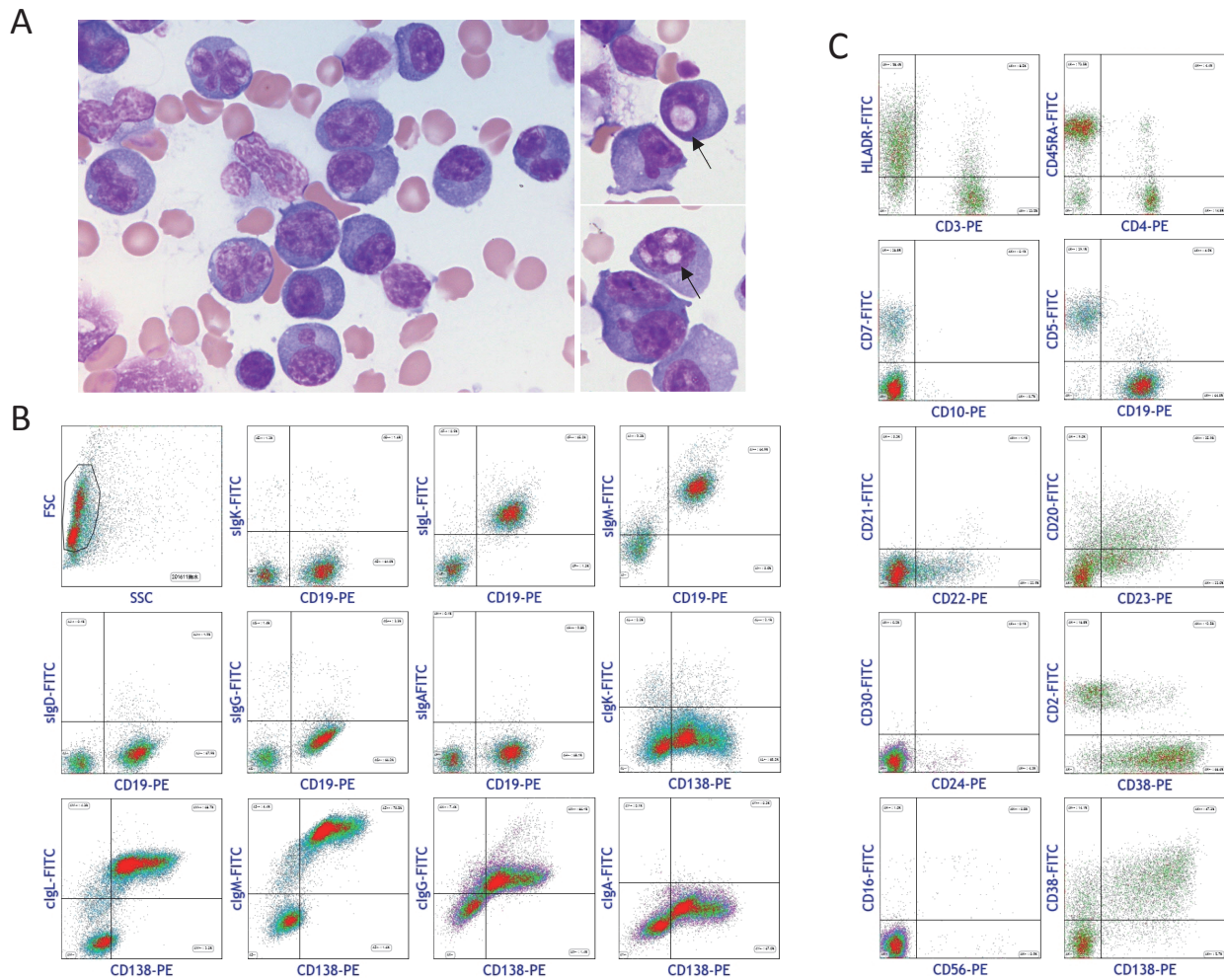


Fig. 2. Cytomorphology and immunophenotype of lymphoma cells. **(A)** May-Giemsa-stained lymphoma cells in pleural fluid, showing a plasmacytic appearance. A few cells had one or more intranuclear inclusions, i.e., Dutcher bodies (*right*, arrows). **(B)** and **(C)** Flow cytometry of pleural fluid cells using antibodies against the antigens indicated. In **B**, cells expressed cell surface and cytoplasmic IgM/ κ monoclonal immunoglobulins. In **C**, cells expressed variable levels of B-cell associated antigens and CD38 and CD138, but lacked myelomatous aberrant expression (e.g. CD56).

Figure S2). We then performed hybridization with the *MALT1* dual-color, break-apart probe and found that add(14) was marked by the green-labeled telomeric probe, representing 3' *MALT1*, while the red-labeled centromeric *MALT1* signal was missing, and, accordingly, interphase nuclei showed the one green and two yellow signal pattern (Figure 3B). The uncharacterized marker chromosome was marked by unrearranged *BCL2* and *MALT1* probes, but not of *IGH*. These cytogenetic studies indicated that the add(14) chromosome represented der(14)t(14;18)(q32;q21), at which the *MALT1-IGH* fusion gene was localized, while the reciprocal der(18)t(14;18)(q32;q21) was deleted.

Amplification and sequencing of the t(14;18)(q32;q21)/MALT1-IGH junction

Since the t(14;18)(q32;q21)/*MALT1-IGH* fusion gene was suggested, DNA extracted from pleural fluid cells was subjected to a long-distance polymerase chain reaction (LD-PCR) in order to amplify the junction encompassing the two genes. PCR primers were designed for *MALT1* exon 1

and for the $E\mu$ enhancer as well as the $C\mu$, $C\gamma$, and $C\alpha$ constant genes of *IGH*; the *MALT1* probe and *IGH* probes were oriented in the opposite direction (Figures 4A and B, Supplementary Table S1). As shown in Figure 4C, we obtained LD-PCR products by the *MALT1-E μ* and *MALT1-C γ* primer combination, indicating $C\mu$ to $C\gamma$ class switching. Nucleotide sequencing of the *MALT1-E μ* product revealed that the junction occurred at the J6 segment of *IGH* and the nucleotide position -5,399 of adenine of the ATG start codon of *MALT1* at the position +1, and a fragment of 9 base pairs (bp) in length was inserted at the junction (Figures 4A and D). As a result of translocation, the *MALT1* and *IGH* $E\mu$ - $C\gamma$ segments were aligned in the divergent transcriptional orientation. Reverse-transcriptase PCR confirmed the expression of *MALT1* in pleural fluid cells, even though the level was lower than those of *in vitro* cultured lymphoma cell lines (Supplementary Figure S3).

We then applied LD-PCR using the *MALT1-E μ* primer combination to another case with t(14;18) reported previously by us.⁷ The sequences encompassing the *MALT1-IGH*

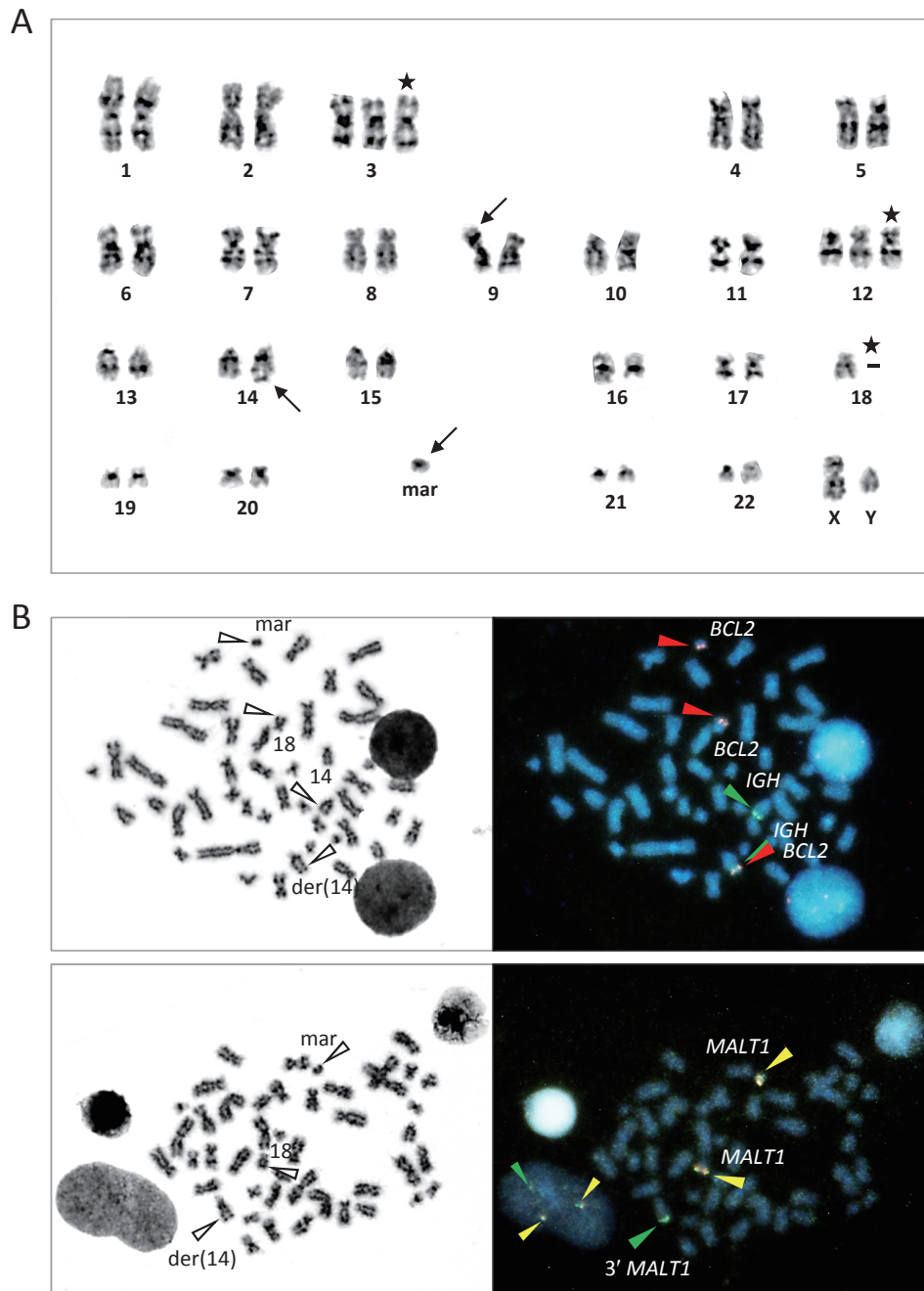


Fig. 3. Cytogenetic studies. (A) G-banding karyotype. Structural and numerical abnormalities are indicated by arrows and asterisks, respectively. The karyotype is described in the text. (B) FISH of metaphase spreads using the Vysis *BCL2-IGH* dual-color dual fusion probe (top) and Vysis *MALT1* dual-color break-apart probe (bottom). The G-banding spread and FISH image through a triple-band pass filter are aligned. Probes were purchased from Abbott Laboratories, Abbott Park, IL, USA.

junction were composed of the J4 segment, a 46-bp insertion fragment, and the upstream sequences of *MALT1* at the position -1,738 of the start codon (Figures 4A and D).

Treatment course

The patient was treated with 6 cycles of the DRP (dexamethasone, rituximab, and cyclophosphamide) regimen every 21 days.⁸ This led to the resolution of pleural effusion, the disappearance of lymphoma cell invasion in the bone

marrow, and accumulation of the tracer within the lung lesion by FDG-PET/CT. However, the serum IgM/ λ M protein remained detectable by immunofixation and the level of serum IgM remained higher than the normal range.

DISCUSSION

We herein described an elderly man who presented with macroglobulinemia and the unilateral accumulation of pleural

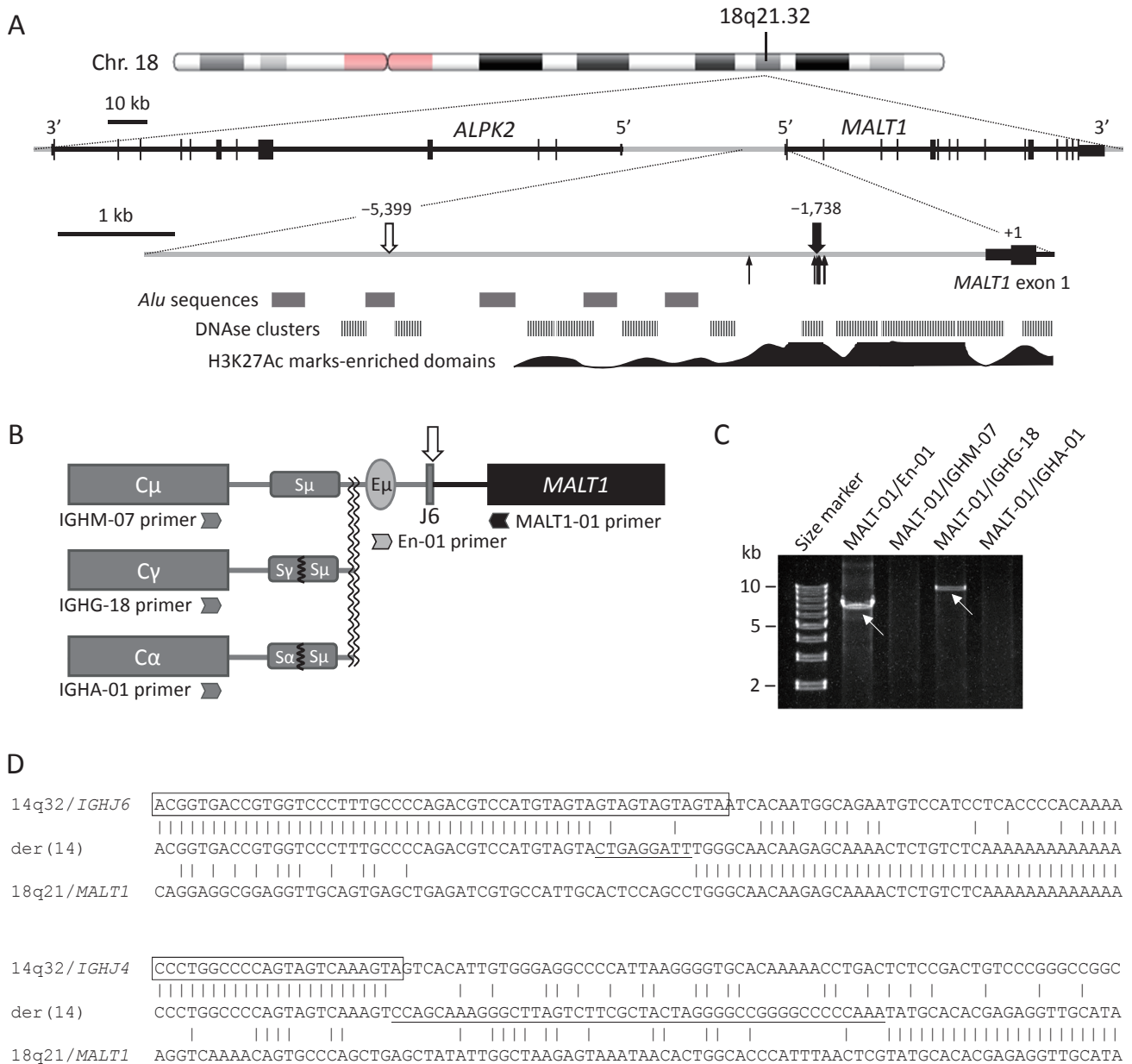


Fig. 4. LD-PCR of the *MALT1-IGH* fusion gene. **(A)** Genomic structure of the *MALT1* gene, which is located at the sub-band 18q21.32 and is oriented from centromere to telomere. The positions of 8 reported breakpoints are indicated by arrows, demonstrating the breakpoint cluster.^{16,17,21} Open and closed arrows indicate the breakpoint of the current case and that of Gomyo *et al.*,⁷ respectively. **(B)** Schematic diagram of LD-PCR of the *MALT1-IGH* junction. The sequences of the primers are described in Supplementary Table S1. **(C)** Ethidium bromide-stained gel electrophoresis of LD-PCR, showing 7.2- and 11-kb products. **(D)** Nucleotide sequences of the t(14;18)(q32;q21)/*MALT1-IGH* junction of the present case (*top*) and those of Gomyo *et al.* (*bottom*). Vertical lines indicate nucleotide identity. The J6 and J4 segments of *IGH* are boxed and *de novo* nucleotide additions are underlined.

fluid. Lymphoma cells in the fluid showed a plasma cell cytomorphology and expressed CD38 and CD138 antigens, but lacked myelomatous antigen aberrations. Most importantly, cytogenetic studies suggested t(14;18)(q32;q21), leading to the generation of the fusion of the *MALT1* gene with *IGH*, and the *MALT1-IGH* junction was confirmed by LD-PCR, which we developed to amplify long DNA targets.^{9,10} Since t(14;18)(q32;q21)/*MALT1-IGH* has been described in a fraction of cases with MALT lymphoma arising in the lung,^{4,11} and because an infiltrative condition of the

ipsilateral lung parenchyma was suggested by imaging studies, we propose that this case represents an extreme form of the plasmacytic differentiation of pulmonary EMZL/MALT lymphoma.

The plasmacytic differentiation of lymphoma cells in association with or without macroglobulinemia may occur in most small B-cell lymphomas, including WM/LPL, chronic lymphocytic leukemia/small lymphocytic lymphoma, follicular lymphoma, mantle cell lymphoma (MCL), and EMZL/MALT lymphoma; however, it varies from being uniformly

present, as in WM/LPL, to very uncommon, as in MCL.⁶ Furthermore, the extent of plasmacytic differentiation may vary from minimal to very extensive, resulting in a resemblance to plasmacytoma in extreme cases.^{4,6,12} Thus, plasmacytic differentiation does not define any specific type of small B-cell lymphoma. Since the *MYD88* L265P somatic mutation is found in most patients with WM/LPL, it has had a significant impact on the differential diagnosis of small B-cell lymphomas; however, this mutation is not entirely specific to WM/LPL and not required for a diagnosis.^{2,6} In contrast, translocations involving *MALT1*, *BCL10*, *FOXP1*, and *GPR34* are exclusively associated with EMZL/MALT lymphoma;^{4,11,13,14} therefore, the detection of these translocations by G-banding, FISH, or appropriate molecular methods is of value for a diagnosis.¹⁵ However, the frequencies of each translocation markedly vary with the primary site of disease and not all tumors carry a translocation; the frequency of t(14;18)(q32;q21) in EMZL/MALT lymphoma arising in the lung ranges between 6 and 10%.^{4,11} Thus, cytogenetic/molecular studies are currently insufficient to effectively discriminate each small B-cell lymphoma category, and the combination of cytomorphological, phenotypic, and sometimes clinical findings is still required in the differential diagnosis of small B-cell lymphomas.

t(14;18)(q32.33;q21.32)/*MALT1-IGH* shares molecular anatomical features with those of t(14;18)(q32.33;q21.33)/*BCL2-IGH*, in that both occur at the J segments of *IGH*,¹⁶ *de novo* nucleotide additions are identified at both breakpoint junctions,^{17,18} and breakpoints within the *BCL2*-major breakpoint cluster and *MALT1* cluster are in close proximity to CpG.¹⁹ Thus, the two translocations may be mediated by the VDJ recombination process of *IGH* and the CpG-type double-strand breakage mechanism proposed by Lieber *et al.*,²⁰ even though, in contrast to the same transcriptional orientation of *BCL2-IGH* joining, *MALT1-IGH* joins in the divergent orientation.¹⁶ We herein found that the breakpoint of the present case was positioned at 3.7 kilo-base pairs (kb) upstream of the *MALT1* breakpoint cluster, which is located 1.7-kb upstream of the *MALT1* start codon,^{16,17,21} while that of the other case fell within the cluster (Figure 4A). Thus, *MALT1* breakpoints may not only be clustered, but also distributed outside the cluster, as observed in *BCL2* breakpoints.¹⁰ Furthermore, we found that the constant gene was class-switched from C μ to C γ , which is another feature frequently observed in the *BCL2-IGH* fusion gene.¹⁰

Although radiotherapy is a treatment of choice for limited-stage EMZL/MALT lymphoma, single-agent rituximab is generally offered to patients with EMZL/MALT lymphoma primarily arising in the lung,²² and radiotherapy is avoided because of the long-term morbidity associated with damage to normal lung tissue. The DRC regimen, which is a combination of rituximab and a cytotoxic agent, was initially developed for patients with WM, showing an overall survival rate of 83% and median progression-free survival of 35 months in a phase II trial.⁸ Since the present patient responded well to and tolerated the treatment, this regimen may be applied to advanced-stage EMZL/MALT lymphoma.

CONFLICT OF INTEREST

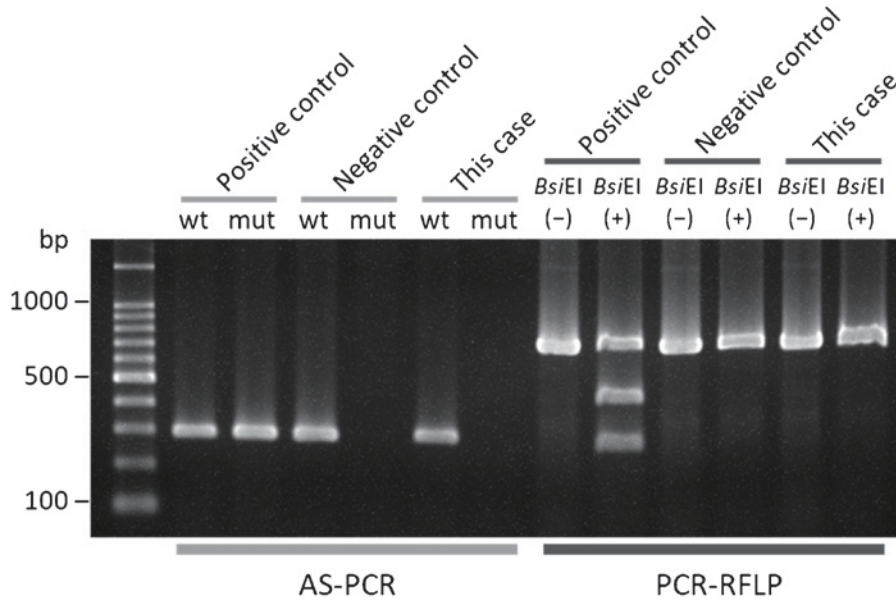
The authors declare no conflict of interest.

REFERENCES

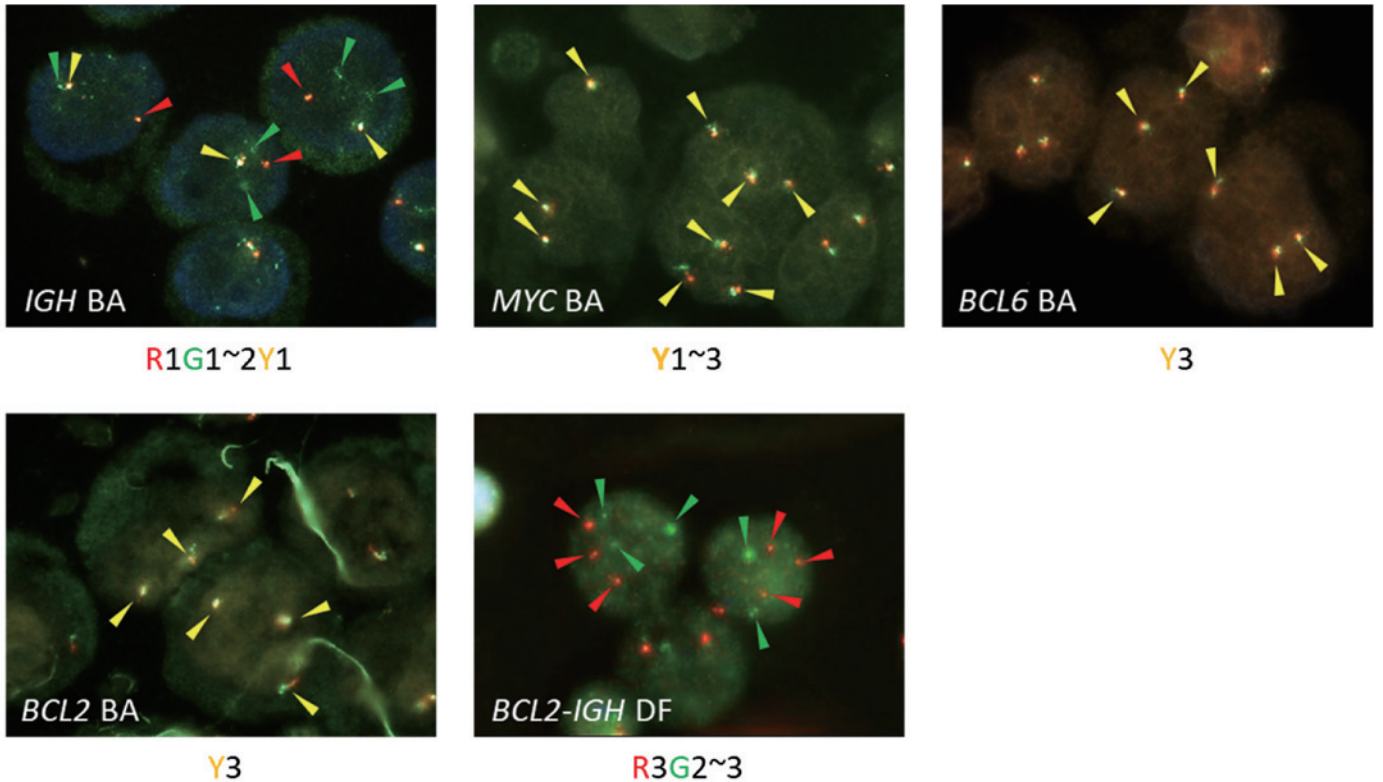
- Owen RG, Treon SP, Al-Katib A, *et al.* Clinicopathological definition of Waldenstrom's macroglobulinemia: consensus panel recommendations from the Second International Workshop on Waldenstrom's Macroglobulinemia. *Semin Oncol.* 2003; 30 : 110-115.
- Swerdlow SH, Cook JR, Sohani AR, *et al.* Lymphoplasmacytic lymphoma. In: Swerdlow SH, Campo E, Harris NL, *et al.* (eds). WHO Classification of Tumours of Haematopoietic and Lymphoid Tissues. Revised 4th edition, Lyon, IARC. 2017; pp. 232-235.
- Min C, Higuchi T, Koyamada R, *et al.* Pulmonary extranodal marginal zone lymphoma with macroglobulinemia and mixed cryoglobulinemia developed in a patient with chronic Hepatitis C. *Intern Med.* 2015; 54 : 2061-2064.
- Cook JR, Isaason PG, Chott A, *et al.* Extranodal marginal zone lymphoma of mucosa-associated lymphoid tissue (MALT lymphoma). In: Swerdlow SH, Campo E, Harris NL, *et al.* (eds). WHO Classification of Tumours of Haematopoietic and Lymphoid Tissues. Revised 4th edition, Lyon, IARC. 2017; pp. 259-262.
- Wohrer S, Streubel B, Bartsch R, *et al.* Monoclonal immunoglobulin production is a frequent event in patients with mucosa-associated lymphoid tissue lymphoma. *Clin Cancer Res.* 2004; 10 : 7179-7181.
- Swerdlow SH, Kuzu I, Dogan A, *et al.* The many faces of small B cell lymphomas with plasmacytic differentiation and the contribution of *MYD88* testing. *Virchows Arch.* 2016; 468 : 259-275.
- Gomyo H, Kajimoto K, Maeda A, *et al.* t(14;18)(q32;q21)-bearing pleural MALT lymphoma with IgM paraproteinemia: value of detection of specific cytogenetic abnormalities in the differential diagnosis of MALT lymphoma and lymphoplasmacytic lymphoma. *Hematology.* 2007; 12 : 315-318.
- Kastritis E, Gavriatopoulou M, Kyrtsionis MC, *et al.* Dexamethasone, rituximab, and cyclophosphamide as primary treatment of Waldenstrom macroglobulinemia: final analysis of a phase 2 study. *Blood.* 2015; 126 : 1392-1394.
- Akasaka T, Akasaka H, Ohno H. Polymerase chain reaction amplification of long DNA targets: application to analysis of chromosomal translocations in human B-cell tumors (review). *Int J Oncol.* 1998; 12 : 113-121.
- Akasaka T, Akasaka H, Yonetani N, *et al.* Refinement of the *BCL2*/immunoglobulin heavy chain fusion gene in t(14;18)(q32;q21) by polymerase chain reaction amplification for long targets. *Genes Chromosomes Cancer.* 1998; 21 : 17-29.
- Remstein ED, Dogan A, Einerson RR, *et al.* The incidence and anatomic site specificity of chromosomal translocations in primary extranodal marginal zone B-cell lymphoma of mucosa-associated lymphoid tissue (MALT lymphoma) in North America. *Am J Surg Pathol.* 2006; 30 : 1546-1553.
- Binesh F, Akhavan A, Navabii H. Extranodal marginal zone B

- cell lymphoma of MALT type with extensive plasma cell differentiation in a man with Hashimoto's thyroiditis. *BMJ Case Rep.* 2011; doi:10.1136/bcr.05.2011.4277. <http://doi.org/10.1136/bcr.05.2011.4277>, (cited 2018-07-26).
- 13 Akasaka T, Lee YF, Novak AJ, *et al.* Clinical, histopathological, and molecular features of mucosa-associated lymphoid tissue (MALT) lymphoma carrying the t(X;14)(p11;q32)/GPR34-immunoglobulin heavy chain gene. *Leuk Lymphoma.* 2017; 58 : 1-4.
 - 14 Murga Penas EM, Hinz K, Roser K, *et al.* Translocations t(11;18)(q21;q21) and t(14;18)(q32;q21) are the main chromosomal abnormalities involving *MLT/MALT1* in MALT lymphomas. *Leukemia.* 2003; 17 : 2225-2229.
 - 15 Ye H, Chuang SS, Dogan A, *et al.* t(1;14) and t(11;18) in the differential diagnosis of Waldenstrom's macroglobulinemia. *Mod Pathol.* 2004; 17 : 1150-1154.
 - 16 Akyuz N, Albert-Konetzny N, Pott C, *et al.* *MALT1* sequencing analyses in marginal zone B-cell lymphomas reveal mutations in the translocated *MALT1* allele in an *IGH-MALT1*-positive MALT lymphoma. *Leuk Lymphoma.* 2017; 58 : 2480-2484.
 - 17 Murga Penas EM, Callet-Bauchu E, Ye H, *et al.* The t(14;18)(q32;q21)/*IGH-MALT1* translocation in MALT lymphomas contains templated nucleotide insertions and a major breakpoint region similar to follicular and mantle cell lymphoma. *Blood.* 2010; 115 : 2214-2219.
 - 18 Jager U, Bocskor S, Le T, *et al.* Follicular lymphomas' BCL-2/IgH junctions contain templated nucleotide insertions: novel insights into the mechanism of t(14;18) translocation. *Blood.* 2000; 95 : 3520-3529.
 - 19 Tsai AG, Lu Z, Lieber MR. The t(14;18)(q32;q21)/IGH-MALT1 translocation in MALT lymphomas is a CpG-type translocation, but the t(11;18)(q21;q21)/API2-MALT1 translocation in MALT lymphomas is not. *Blood.* 2010;115:3640-3641; author reply 3641-3642.
 - 20 Lieber MR. Mechanisms of human lymphoid chromosomal translocations. *Nat Rev Cancer.* 2016; 16 : 387-398.
 - 21 Sanchez-Izquierdo D, Buchonnet G, Siebert R, *et al.* *MALT1* is deregulated by both chromosomal translocation and amplification in B-cell non-Hodgkin lymphoma. *Blood.* 2003; 101 : 4539-4546.
 - 22 Okamura I, Imai H, Mori K, *et al.* Rituximab monotherapy as a first-line treatment for pulmonary mucosa-associated lymphoid tissue lymphoma. *Int J Hematol.* 2015; 101 : 46-51.

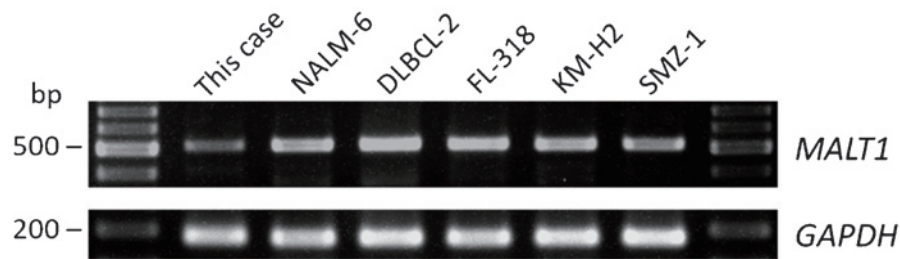
Supplementary Materials



Supplementary Fig. S1. Allele-specific (AS-) PCR and PCR-RFLP assays detecting *MYD88* L265P mutation. For AS-PCR, wild-type (wt) and mutated (mut) alleles were assayed in each sample and the PCR products were electrophoresed side-by-side, and for PCR-RFLP, *BsiEI*-undigested [*BsiEI*(-)] and *BsiEI*-digested [*BsiEI*(+)] PCR products were electrophoresed side-by-side on a 2% agarose gel. A sample from a case with WM was used as a positive control and a healthy volunteer was used as a negative control.



Supplementary Fig. S2. FISH of interphase nuclei, showing rearrangement of *IGH* and the lack of rearrangement of *BCL2*, *BCL6*, and *MYC*. Cytospin smear slides or chromosome preparations were hybridized with the dual-color, break-apart (BA) probes for *IGH*, *MYC*, *BCL6*, and *BCL2* genes, and the *BCL2-IGH* dual-color dual-fusion (DF) probe. Hybridization signals are indicated by arrow heads of each color and the pattern of hybridization signals is summarized at the bottom of each picture (R, red signal; G, green signal; Y, yellow signal). The probes were purchased from Abbott Laboratories, Abbott Park, IL, USA.



Supplementary Fig. S3. Revers-transcriptase (RT-) PCR for the expression of *MALT1* mRNA. The hematological tumor cell lines used as expression controls were: NALM-6, pre-B acute lymphoblastic leukemia; DLBCL-2, diffuse large B-cell lymphoma; FL-318, follicular lymphoma; KM-H2, Hodgkin lymphoma; and SMZ-1, peripheral T-cell lymphoma. RT-PCR for *GAPDH* is shown in the bottom to confirm that similar amounts of mRNA were loaded. The sequences of the primers for RT-PCR are described in Supplementary Table S1.

Supplementary Table S1. Sequences of the PCR primers used for LD-PCR of t(14;18)(q32;q21)/*MALT1-IGH*, RT-PCR of *MALT1* and *GAPDH*, and AS-PCR and PCR-RFLP of *MYD88* L265P mutation

Designation	Sequence (5' to 3')	Size of PCR product
LD-PCR of t(14;18)(q32;q21)/ <i>MALT1-IGH</i>		
IGHM-07	CAGAATGGCTGAGGGCTCAGGTTTGGGTGGACCAG	NA
IGHG-18	GGCCTTCTCGGCCACCAGCCACCTCCTCCCTCTC	NA
IGHA-01	TTCGTGTAGTGCTTCACGTGGCATGTCACGGACTT	NA
En-01	CTAGGCCAGTCCTGCTGACGCCGCATCGGTGATTC	NA
MALT1-01	CGAGGGCGGCAGGGCCTGTAGCGGGTCCCCAACA	NA
RT-PCR of <i>MALT1</i> and <i>GAPDH</i>		
MALT1-forward	GCGGAGCTGGCGGGGAGTCG	511 bp
MALT1-reverse	GCAACTTGGATTACAGAGACG	
GAPDH-forward	GACATCAAGAAGGTGGTGAA	178 bp
GAPDH-reverse	TGTCATACCAGGAAATGAGC	
AS-PCR and PCR-RFLP of <i>MYD88</i> L265P mutation		
MYW-F (wild type)	GTGCCCATCAGAAGCGCCT	296 bp
MYM-F (mutant)	GTGCCCATCAGAAGCGCCC	296 bp
MY-F	GGGATATGCTGAACTAAGTTGCCAC	726 bp
MY-R	GACGTGTCTGTGAAGTTGGCATCTC	

NA, not applicable

METHODS

Flow cytometry

Cells prepared from the pleural fluid were subjected to cell-surface and cytoplasmic antigen analysis using a flow cytometer. Cell distribution was examined in forward versus side scatter cytograms by setting multiple gates, and antigen expression of gated cells was analyzed by multicolor flow cytometry.

Allele-specific (AS-) PCR and PCR-RFLP for *MYD88* L265P mutation

For AS-PCR, two forward primers were designed to differentiate the wild-type and mutated alleles of *MYD88* L265P. To optimize the specificity, an internal mismatch in the third position from the 3' end was introduced. The sequences of the primers and those of the reverse primer are described in Supplementary Table S1. For PCR-RFLP, PCR

amplifying a 726-bp fragment of *MYD88* exon 5 was first performed using the primer combination described in Supplementary Table S1 and the amplified fragment was then subjected to *Bsi* EI restriction enzyme digestion for 15 minutes at 60°C. The mutated allele contains a *Bsi* EI site resulting in 448-bp and 278-bp fragments, whereas the wild-type allele does not. All PCR procedures were carried out in a Veriti 96 Well Thermal Cycler (Applied Biosystems, Inc., Forester City, CA, USA).

Cytogenetic analysis

Cells prepared from the pleural fluid were incubated overnight under the standard condition, and then cultured in the presence of 0.1 µg/mL colcemid for 2 hr. After harvesting, the cells were treated with hypotonic solution and fixed in methanol:acetic acid (3:1). Chromosomes were banded by trypsin-Giemsa staining and the results of the chromosome analysis were described according to the ISCN 2016.

FISH

The Vysis FISH probe were purchased from Abbott Laboratories, Abbott Park, IL, USA. Denaturing of the chromosome/probe, hybridization, and washing conditions were as recommended by the manufacturer. FISH results were analyzed by a fluorescence microscope (Nikon Corporation, Tokyo, Japan) equipped with DAPI, fluorescein isothiocyanate (FITC), and tetramethylrhodamine B isothiocyanate (TRITC) fluorescence filters, as well as a DAPI/FITC/TRITC triple band-pass filter (Nikon Corporation).

LD-PCR encompassing the MALT1-IGH fusion gene

Genomic DNA was isolated from the pleural fluid cells by means of proteinase K and phenol/chloroform, and subjected to LD-PCR encompassing the t(14;18)(q32;q21)/*MALT1-IGH* junction. The sequences of the primers are described in Supplementary Table S1. PCR amplification

was performed in a Veriti 96 Well Thermal Cycler (Applied Biosystems, Inc., Forester City, CA, USA). PCR products were visualized by ethidium bromide-stained agarose gel electrophoresis, excised from the gel, and cloned into the plasmid (pGEM®-T Easy, Promega). In order to avoid PCR artifacts, three independent cloned DNAs were sequenced by an ABI 310 automated sequencer (Applied Biosystems).

Reverse transcriptase (RT-) PCR

Total cellular RNA was prepared with an RNeasy Mini Kit (QIAGEN, Hilden Germany). First strand cDNA was synthesized from 2 µg of total RNA in the reaction mixture containing random hexamer primers (Roche Applied Science, Penzberg, Germany) and SuperScript® reverse transcriptase (Invitrogen, Carlsbad, CA). PCR primers for RT-PCR and the size of the products were listed in Supplementary Table S1.